LAWRENCE
LIVERMORE
NATIONAL
LABORATORY

LLNL-JRNL-654915

In situ TEM investigation of the interfacial reaction between Ni and Al during rapid heating in a nanocalorimeter

M. D. Grapes, T. LaGrange, K. Woll, B. W. Reed, G. H. Campbell, D. A. LaVan, T. P. Weihs

May 27, 2014

APL Materials

Disclaimer

In situ TEM investigation of the interfacial reaction between Ni and Al during rapid heating in a nanocalorimeter

Michael D. Grapes[1,2,a)], Thomas LaGrange[3], Karsten Woll[1,4], Bryan W. Reed[3], Geoffrey H. Campbell[3], David A. LaVan[2,b)], and Timothy P. Weihs[1,c)]

[1] *Department of Materials Science and Engineering, Johns Hopkins University, Baltimore, Maryland 21218, USA*

[2] *Materials Measurement Science Division, Material Measurement Laboratory, National Institute of Standards and Technology, Gaithersburg, Maryland 20899, USA*

[3] *Condensed Matter and Materials Division, Lawrence Livermore National Laboratory, Livermore, California 94550, USA*

[4] *Institute of Applied Materials, Karlsruhe Institute of Technology, 76344 Eggenstein-Leopoldshafen, Germany*

[a)] mike.grapes@gmail.com, [b)] david.lavan@nist.gov, [c)] weihs@jhu.edu

Abstract

The Al/Ni formation reaction is highly exothermic and of both scientific and technological significance. In particular, Al/Ni thin-film multilayers have been used as a model system to understand how steep concentration gradients and large heating rates affect the identity and sequence of phases that form at the interface between two materials. Historical studies of the Al/Ni interfacial reaction at heating rates below 1 K/s show that the phase transformation sequence starts with the most Al-rich phase and proceeds through progressively more Ni-rich phases. Here, we present the phase transformation sequence that is observed when the heating rate is increased to 830 K/s. Single 100 nm Al/Ni bilayers were deposited onto nanocalorimeter sensors that enable the measurement of temperature and heat flow at heating rates up to 100,000 K/s. The nanocalorimeter sensors were placed in a custom-built *in situ* transmission electron microscope (TEM) stage and heated rapidly while measuring the heat flow and acquiring TEM electron diffraction patterns. Heat flow measurements show a sequence of three exothermic peaks during the heating experiment and a total heat release of 1307 J/g $\pm$ 43 J/g. The electron diffraction patterns captured simultaneously with the thermal measurements allow us to identify the intermetallic phases present and reconstruct the phase transformation sequence as a function of time and temperature. The results reveal that at this heating rate the overall phase transformation sequence is not altered compared to that at lower rates. Based on these results, *in situ* nanocalorimetry promises to be a valuable tool for the investigation of thermally activated dynamic phenomena.

Thin film and interfacial reactions have been studied extensively for many years. These reactions are of broad interest both in industry (e.g. for microelectronics[1,2], MEMS[3,4], and coatings[5]) and in science, where reduced diffusion distances and increased surface energy provide an opportunity to study phase formation in a unique environment[6–9]. One of the best characterized thin film reactions is between Al and Ni[10–20]. Al and Ni have a large, negative heat of mixing, making the reaction highly exothermic. Multilayer foils consisting of nanoscale layers of Al and Ni can release this energy very quickly. When a multilayer foil is ignited at one end in a free-standing configuration, the heat released locally is sufficient to ignite the adjacent material and produce a high-velocity reaction front in what is known as a "self-propagating" reaction. Heating rates when reacting in this mode exceed 10^6 K/s. Because of their ability to deliver rapid, local heating, Al/Ni multilayer foils have been exploited extensively as heat sources for rapid room-temperature soldering[11–13].

In order to better understand the reaction in Al/Ni multilayers, many studies have identified the sequence of phases that form as the multilayers are heated[14–17]. Historically, these studies have been accomplished using differential scanning calorimetry (DSC) or differential thermal analysis (DTA). These instruments heat a sample at a controlled rate that is typically less than 1 K/s and measure the heat evolved as a function of temperature. The phase(s) present at different points during the heating cycle are determined by quenching and analyzing the sample with x-ray diffraction (XRD). More recently, there has been interest in studying the phase transformations during self-propagation of these reactions, where heating rates are approximately one-million times higher. Since quenching is difficult for reactions progressing at these rates, *in situ* characterization methods are preferred in this regime. To-date such studies have been accomplished using two techniques: synchrotron x-ray microdiffraction[18,19] and time-resolved transmission electron microscopy[20].

For multilayers with a 1:1 Al:Ni atomic ratio, slow heating experiments typically have identified two phase transformation sequences depending on the deposition method. For evaporated Al/Ni multilayers[14,21], the phase transformation sequence under slow heating is

$$\mathrm{Al} + \mathrm{Ni} \rightarrow \mathrm{Al_3Ni} + \mathrm{Ni} \rightarrow \mathrm{Al_3Ni_2} + \mathrm{Ni} \rightarrow \mathrm{AlNi} \qquad (1)$$

For Al/Ni multilayers that are deposited by sputtering or ion-beam deposition the sequence is altered slightly[15,17]:

$$Al + Ni \rightarrow Al_9Ni_2 + Ni \rightarrow Al_3Ni + Ni \rightarrow Al_3Ni_2 + Ni \rightarrow AlNi \qquad (2)$$

The distinction between these two sequences is in the first phase to form and is attributed to subtle differences in the initial microstructure of the as-deposited Al/Ni interfaces. These interfaces tend to be more intermixed in sputtered and ion-beam deposited samples, which in turn can impact the nucleation of the Al_9Ni_2 and Al_3Ni phases which have similar free energies of formation[17].

When sputter deposited Al/Ni multilayers are reacted in the rapid, self-propagating mode (heating rates exceeding 10^6 K/s) and characterized using synchrotron x-ray diffraction[18,19] or time-resolved TEM[20], the observed phase transformation sequence becomes

$$Al + Ni \rightarrow \text{Al-rich liquid} + Ni \rightarrow AlNi \qquad (3)$$

Note that while at low heating rates we observe a sequence of solid intermetallic phases, at high heating rates all of the intermetallic phases are skipped and instead mixing occurs in a molten Al-rich phase. The shift in phase sequence with heating rate is attributed to a reduction in the amount of atomic intermixing that occurs prior to reaching temperatures where the intermediate intermetallic phases are no longer stable[18]. To-date this characterization has only been performed on sputtered Al/Ni multilayers, but evaporated multilayers are likely to exhibit the same sequence given that the vast majority of mixing occurs through Ni dissolving into molten Al.

To study this phenomenon over a broad range of heating rates this work seeks to demonstrate that one can characterize the AlNi formation reaction at heating rates in the 10^3 K/s to 10^5 K/s range, intermediate between the heating rates in DSC studies and in self-propagating reactions. Given that these heating rates are orders of magnitude larger than what is possible using a standard DSC, we employ a calorimetric technique that is capable of more rapid heating: nanocalorimetry. A nanocalorimeter is a MEMS device whose miniscule heat capacity enables it to achieve very high heating rates[22]. However, as in self-propagating reactions, analyzing the phases formed at these heating rates is difficult using quenching and *ex situ* observations. Thus, an *in situ* approach is preferred so that phases can be detected as they appear. In this work we utilize a newly developed *in situ* nanocalorimetry system[23] that makes use of the dynamic

transmission electron microscope (DTEM[24]) to perform structural characterization during the calorimetry experiment. The DTEM is a time-resolved TEM designed, built, and housed at Lawrence Livermore National Laboratory.

The *in situ* nanocalorimetry system is depicted schematically in Fig. 1 and consists of the DTEM itself, TEM-compatible nanocalorimeter sensors, an *in situ* nanocalorimetry TEM holder, and a data acquisition system. The DTEM utilizes a UV-laser-driven photocathode to produce extremely short, high intensity electron pulses[24]. The laser intensity and duration can be manipulated to create electron pulses from 30 ns to 500 ns in length. Nanocalorimeters consist of a platinum strip for heating and temperature measurement suspended on a silicon nitride membrane to minimize heat losses and thermal mass[22]. The temperature-resistance relationship for each sensor is calibrated optically[25] prior to first use, and for DTEM investigation the sensor design was modified to include three 100 μm x 100 μm electron-transparent windows in the platinum strip[23]. After a sample is deposited on the sensor it is placed into a custom-built *in situ* nanocalorimetry holder which is compatible with the DTEM goniometer. This holder provides electrical connections between the Pt sensor and a data acquisition system that is synchronized with the DTEM via a custom-built LabVIEW interface. Full details on the design and operation of the *in situ* nanocalorimetry system have been reported elsewhere[23].

The samples tested in this study were single-bilayer analogs of standard Al/Ni multilayers consisting of 40 nm of Ni (target purity 99.995 %) sandwiched between two 30 nm layers of Al (target purity 99.999 %) for a total bilayer thickness of 100 nm and an overall composition of 50 atomic percent of Al. 10 nm of Al_2O_3 was deposited on both sides of the Al/Ni/Al stack to serve as a passivation layer and diffusion barrier. This sample geometry is illustrated in the upper-left of Fig. 1. The sample stack was deposited through a shadow-mask directly onto the underside of the nanocalorimeter sensor by e-beam evaporation. Layer thickness during deposition was measured by a quartz crystal thickness monitor. For the experiments reported here, the DTEM was configured for single-shot mode with an electron-pulse-duration of 500 ns. Selected-area electron diffraction patterns were collected with a ≈ 0.55 μm^2 selected-area aperture positioned in the central electron window of the nanocalorimeter heater strip. Since the Al/Ni formation reaction is irreversible, four nanocalorimeters containing identical samples were reacted and

imaged at different times to construct a full picture of the phase formation sequence. The average heating rate during the experiments was 830 K/s.

Characteristic results from the nanocalorimetry system during the heating segment of one experiment are presented in Fig. 2. The plot of temperature vs. time in Fig. 2a depicts the measurable difference in the temperature evolution of the sample during the first heating (when a reaction is occurring) as compared to the second heating (when the reactants have already been consumed). This difference can be extracted and quantified to give the reaction power, i.e. the rate of heat release that is due to a reaction in the sample and not external heating, shown in Fig. 2b. Note the presence of two large exothermic peaks with one small exothermic peak in between them. These peaks are highlighted by fitting each with a Voigt distribution in Fig. 2b.

Electron diffraction patterns were captured using the DTEM at the times indicated in Fig. 2 in order to identify the phase transformations occurring in each of the three exotherms. In addition to the four electron diffraction patterns captured during the heating experiment (B – E), patterns were also taken at room temperature before (A) and after (F) to identify the initial and final phases. Fig. 3 presents these results as a sequence of 1D diffraction patterns, obtained by rotational averaging of the original 2D patterns followed by background subtraction. All observable peaks are labeled with the most likely phase or phases. We also label the temperature of the sample when the pattern was captured and the amount of heat that had been released up that point (as a percentage of the total theoretical heat of formation for AlNi). The sequence is described briefly below.

Pattern A presents the initial state of the sample prior to heating. All of the measured diffraction peaks can be attributed to either fcc Al or fcc Ni. Pattern B is the first pattern captured during the heating experiment. It represents a 280 K temperature increase over Pattern A but still represents a pre-reaction microstructure (3 % reaction completion). As such, it shows essentially no changes from Pattern A other than slight peak broadening and a slight shift to smaller $1/d$ due to thermal expansion. Pattern C was captured more than half-way through the first exotherm as shown in Fig. 2b. Here we see the first clear evidence of a reaction, as the fcc Al peaks have disappeared and have been replaced by peaks from Al_3Ni ($oP16$ structure[26]). Al_3Ni has an

exceptionally large number of diffraction peaks (over 450 in the range shown) that are too weak to detect in these experiments. However, in certain regions these peaks overlap to give measurable intensities distinct from those of fcc Ni. These regions are labeled in Fig. 3 and include a broad peak around 2.72 nm^{-1} (formed by the (011), (101), (020), (111), and (200) reflections) and a shoulder around 4.07 nm^{-1} (formed by the (211), (220), and (002) reflections). Pattern D represents the state of the sample near the end of the second, small exotherm. Diffraction peaks from Ni and Al_3Ni are still visible, but this pattern shows the first clear evidence for the Al_3Ni_2 phase (*hP*5 structure[26]) in the form of the (001) peak at 2.04 nm^{-1} and the (202)/(022) peak at 7.03 nm^{-1}. There is some evidence for the (100) peak at 2.86 nm^{-1} and the (212)/(122) peak at 8.60 nm^{-1}, but the former is obscured by the nearby Al_3Ni peaks while the latter combines with the shrinking (220) and (311) Ni peaks to form a relatively featureless signal around 8.9 nm^{-1}. In Pattern E, acquired in the middle of the final exotherm, the signal from fcc Ni has almost disappeared except for the shoulder at 5.64 nm^{-1} due to the (200) peak. This makes it easier to see clear peaks due to the Al_3Ni_2 phase. Peaks from AlNi (*cP*2 structure[26]) may also be contributing, but it is very difficult to distinguish between AlNi and Al_3Ni_2 when the peaks are broad unless the AlNi (111) and (210) superlattice peaks at 6.00 nm^{-1} and 7.75 nm^{-1} are visible. This difficulty persists in Pattern F, which shows the final room temperature state of the sample after the heating experiment. There is some evidence for the AlNi superlattice peaks, but the persistence of Al_3Ni_2 peaks suggests that the primary phase is still Al_3Ni_2.

The reaction power in Fig. 2b shows three distinct exotherms. Fitting the exothermic peaks and taking the integral of the cumulative fit curve yields the total heat evolved. Averaged over the four samples reported, the total heat is 1.25 mJ with a standard deviation of 0.042 mJ. The sample mass can be estimated using the intended layer thicknesses, the estimated sample area (3.7 mm x 0.5 mm), and the bulk densities for Al and Ni. We estimate the mass in this way to be 960 ng yielding a normalized average heat of formation of 1302 J g^{-1} $\pm$ 44 J g^{-1}. This is 5.7 % $\mp$ 3.2 % lower than the theoretical value[27], 1381 J g^{-1}. Since Al_3Ni_2 peaks are still visible in the final diffraction pattern an incomplete reaction is likely responsible for at least part of this discrepancy (if the final phase contained no AlNi the theoretical discrepancy would be about 4%). The remainder is likely due to the estimation of the sample mass. Comparing the positions

of the exothermic peaks in Fig. 2 to the electron diffraction patterns in Fig. 3 we can conclude that the first exotherm in the nanocalorimetry data corresponds to the formation of Al_3Ni, the second to the formation of Al_3Ni_2, and the third to growth of Al_3Ni_2 and possibly the formation of AlNi. Comparing this sequence to the one presented in Eq. 1 for evaporated Al/Ni layers under slow heating, the overall phase transformation sequence appears unaltered at a rate of 830 K/s. However, it appears that in these experiments Al_3Ni_2 grows in a two-stage mode, with the small, middle exotherm corresponding to the formation of an interfacial layer of Al_3Ni_2 and the larger final peak corresponding to 1D diffusional growth of this phase. Two-stage growth is not uncommon in Al/Ni multilayers and thin film multilayers in general[14,16,28], and has been reported for the first phase, Al_3Ni. However, these experiments do not support a two-stage growth mode for Al_3Ni, only for the second intermetallic phase, Al_3Ni_2. The difference may be due to the large increase in heating rate compared to earlier studies, but a more comprehensive examination of Al_3Ni formation over a range of heating rates is required to confirm this explanation.

Going forward, one line of investigation will be to extend the present work on the 1:1 Al:Ni composition to higher heating rates where more significant changes in phase formation sequence may occur. However, since characteristic reaction temperatures increase as the heating rate increases[29] there may be a limit on the maximum heating rate that can be studied while still forming the final AlNi phase. In light of this, a second line of investigation will be to study films with the Al-rich compositions of 3:1 and 3:2 Al:Ni (corresponding to the Al_3Ni and Al_3Ni_2 intermetallic phases). By excluding the formation of the highest temperature phase, AlNi, these samples will allow us to study the formation of the Al_3Ni and Al_3Ni_2 intermetallics at heating rates up to the maximum rates possible using nanocalorimetry.

More generally, the *in situ* nanocalorimetry system demonstrated here can be applied to study rapid phase transformations and microstructural changes in a number of fields. The ability to rapidly heat and cool materials while simultaneously characterizing heat flow and sample structure/morphology should aid the study of transformations in phase change materials, amorphization and crystallization in bulk metallic glasses, and grain growth and recrystallization in thin films.

In conclusion, we have demonstrated that one can study rapid phase transformations in 1:1 Al:Ni bilayers using a new *in situ* nanocalorimetry + DTEM system. The intermediate phases in the reaction were identified using *in situ* electron diffraction for samples heated at an average heating rate of 830 K/s. Nanocalorimeter data indicates that at this heating rate, the formation reaction occurs in a sequence of three exotherms and produces the expected heat of formation. Meanwhile, the *in situ* DTEM electron diffraction confirms that the phase transformation sequence is similar to that observed at much slower heating rates in a DSC, i.e. $Al + Ni \rightarrow Al_3Ni + Ni \rightarrow Al_3Ni_2 + Ni \rightarrow AlNi$. Future work on this system will aim to analyze the phase transformation sequence for 1:1 Al:Ni bilayers at higher heating rates, and to study bilayers with 3:1 and 3:2 Al:Ni compositions in order to gain a better understanding of the processes by which the Al_3Ni and Al_3Ni_2 intermetallic phases form.

Acknowledgements

The authors are grateful to Bernadette Cannon for her help calibrating nanocalorimeter sensors during her time as a NIST Summer Undergraduate Research Fellowship (SURF) student. M.D.G. and T.P.W. were supported in part by NIST Grant 70NANB9H9146 and in part by National Science Foundation Grant DMR-1308966. M.D.G., K.W., and T.P.W. were supported in part by U.S. Department of Energy Grant DE-FG02-09ER46648. Nanocalorimeter fabrication was performed at the NIST Center for Nanoscale Science & Technology. The work presented in this article conducted at the LLNL DTEM facility was performed under the auspices of the U.S. Department of Energy by Lawrence Livermore National Laboratory under Contract DE-AC52-07NA27344. The DTEM experiments conducted at LLNL and effort of T.L., B.W.R., and G.H.C. were supported by the U.S. Department of Energy, Office of Basic Energy Sciences, Division of Materials Science and Engineering under FWP SCW0974. Certain commercial equipment, instruments, or materials are identified in this document. Such identification does not imply recommendation or endorsement by the National Institute of Standards and Technology, nor does it imply that the products identified are necessarily the best available for the purpose. Since the completion of this work, T.L. and B.W.R. have become employees at Integrated Dynamic Electron Solutions, Inc., a start-up company marketing time-resolved electron microscope technology.

References

[1] F.M. D'Heurle, J. Mater. Res. **3**, 167 (1988).

[2] R. Rosenberg, D.C. Edelstein, C.-K. Hu, and K.P. Rodbell, Annu. Rev. Mater. Sci. **30**, 229 (2000).

[3] Y. Fu, H. Du, W. Huang, S. Zhang, and M. Hu, Sensors Actuators A Phys. **112**, 395 (2004).

[4] Y. Shacham-Diamand and Y. Sverdlov, Microelectron. Eng. **50**, 525 (2000).

[5] M.J. Pomeroy, Mater. Des. **26**, 223 (2005).

[6] K.F. Kelton and A.L. Greer, *Nucleation in Condensed Matter: Applications in Materials and Biology* (Elsevier, 2010).

[7] U. Gösele and K.N. Tu, J. Appl. Phys. **53**, 3252 (1982).

[8] F. Hodaj and A.M. Gusak, Acta Mater. **52**, 4305 (2004).

[9] R.J. Highmore, Philos. Mag. Part B **62**, 455 (1990).

[10] E.G. Colgan, Mater. Sci. Reports **5**, 1 (1990).

[11] J. Wang, E. Besnoin, A. Duckham, S.J. Spey, M.E. Reiss, O.M. Knio, M. Powers, M. Whitener, and T.P. Weihs, Appl. Phys. Lett. **83**, 3987 (2003).

[12] A.J. Swiston, T.C. Hufnagel, and T.P. Weihs, Scr. Mater. **48**, 1575 (2003).

[13] X. Qiu and J. Wang, Sensors Actuators A Phys. **141**, 476 (2008).

[14] E. Ma, C.V. Thompson, and L.A. Clevenger, J. Appl. Phys. **69**, 2211 (1991).

[15] A.S. Edelstein, R.K. Everett, G.Y. Richardson, S.B. Qadri, E.I. Altman, J.C. Foley, and J.H. Perepezko, J. Appl. Phys. **76**, 7850 (1994).

[16] C. Michaelsen, G. Lucadamo, and K. Barmak, J. Appl. Phys. **80**, 6689 (1996).

[17] K.J. Blobaum, D. Van Heerden, A.J. Gavens, and T.P. Weihs, Acta Mater. **51**, 3871 (2003).

[18] J.C. Trenkle, L.J. Koerner, M.W. Tate, N. Walker, S.M. Gruner, T.P. Weihs, and T.C. Hufnagel, J. Appl. Phys. **107**, 113511 (2010).

[19] K. Fadenberger, I.E. Gunduz, C. Tsotsos, M. Kokonou, S. Gravani, S. Brandstetter, A. Bergamaschi, B. Schmitt, P.H. Mayrhofer, C.C. Doumanidis, and C. Rebholz, Appl. Phys. Lett. **97**, 144101 (2010).

[20] J.S. Kim, T. LaGrange, B.W. Reed, R. Knepper, T.P. Weihs, N.D. Browning, and G.H. Campbell, Acta Mater. **59**, 3571 (2011).

[21] T.S. Dyer and Z.A. Munir, Metall. Mater. Trans. B **26**, 603 (1995).

[22] E.A. Olson, M.Y. Efremov, and L.H. Allen, J. Microelectromechanical Syst. **12**, 355 (2003).

[23] M.D. Grapes, T. LaGrange, B.W. Reed, G.H. Campbell, T.P. Weihs, and D.A. LaVan, Rev. Sci. Instrum. (to be submitted).

[24] B.W. Reed, T. LaGrange, R.M. Shuttlesworth, D.J. Gibson, G.H. Campbell, and N.D. Browning, Rev. Sci. Instrum. **81**, 053706 (2010).

[25] P. Swaminathan, B.G. Burke, A.E. Holness, B. Wilthan, L. Hanssen, T.P. Weihs, and D.A. LaVan, Thermochim. Acta **522**, 60 (2011).

[26] P.V. and L.D. Calvert, *Pearson's Handbook of Crystallographic Data for Intermetallic Phases*, 2nd ed. (ASM International, 1991).

[27] S.H. Fischer and M.C. Grubelich, in *32nd Jt. Propuls. Conf. Exhib.* (American Institute of Aeronautics and Astronautics, Reston, Virigina, 1996).

[28] K.R. Coffey, L.A. Clevenger, K. Barmak, D.A. Rudman, and C.V. Thompson, Appl. Phys. Lett. **55**, 852 (1989).

[29] H.E. Kissinger, Anal. Chem. **29**, 1702 (1957).

Figure Captions

Fig. 1 – Schematic of the experimental system for *in situ* nanocalorimetry showing a nanocalorimeter sensor, the *in situ* nanocalorimetry TEM holder, the dynamic TEM, and the data acquisition system. Also shown is the sample geometry studied in this work, a 100 nm thick Ni/Al bilayer.

Fig. 2 – Typical nanocalorimetry data for a 100 nm Al/Ni bilayer heated at an average rate of 830 K/s: (a) temperature vs. time for two consecutive scans showing the temperature excursion when a reaction occurs, and (b) the reaction power vs. time showing heat evolution in three distinct exothermic peaks fitted with Voigt distributions. The dashed lines indicate the times at which the diffraction patterns in Fig. 3 were taken.

Fig. 3 – DTEM electron diffraction patterns captured before, during, and after the reaction of a 100 nm Al/Ni bilayer. The pattern labels correspond to those in Fig. 2. Also labeled for each pattern are the percentage of heat released (as a fraction of the theoretical enthalpy of formation) and the temperature when the pattern was captured.

Figures

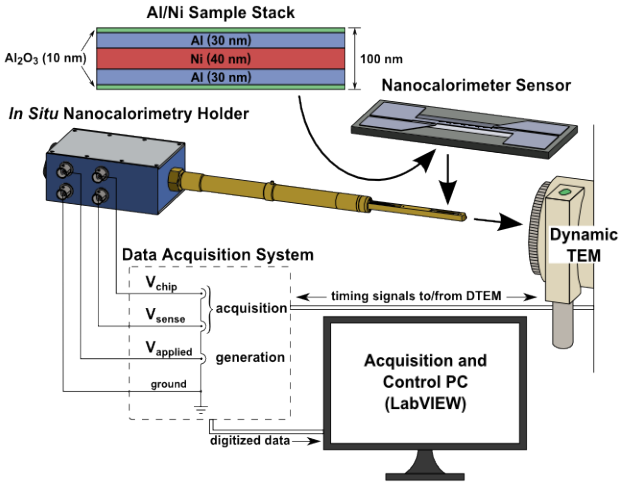

Fig. 1 – Schematic of the experimental system for *in situ* nanocalorimetry showing a nanocalorimeter sensor, the *in situ* nanocalorimetry TEM holder, the dynamic TEM, and the data acquisition system. Also shown is the sample geometry studied in this work, a 100-nm-thick Ni/Al bilayer.

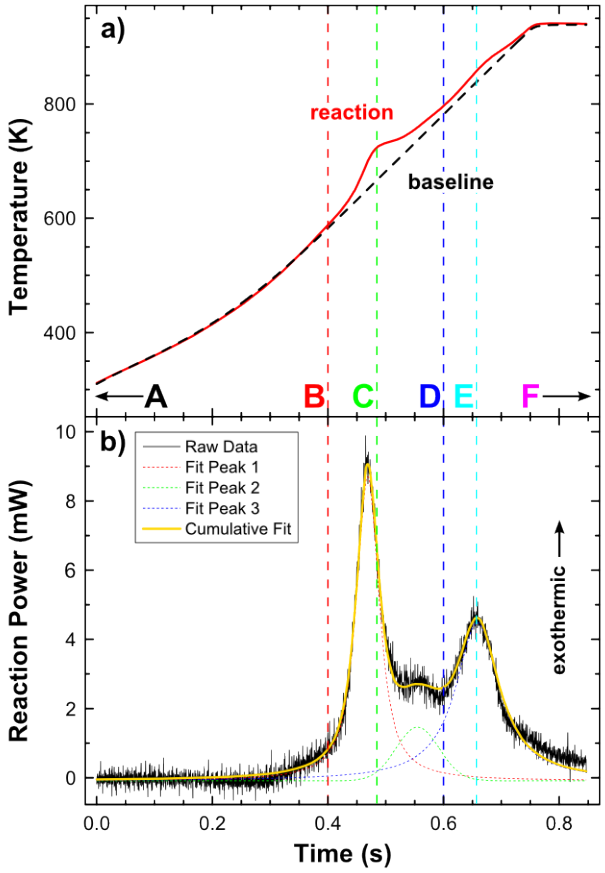

Fig. 2 – Typical nanocalorimetry data for a 100 nm Al/Ni bilayer heated at an average rate of 830 K/s: (a) temperature vs. time for two consecutive scans showing the temperature excursion when a reaction occurs, and (b) the reaction power vs. time showing heat evolution in three distinct exothermic peaks. The dashed lines indicate the times at which the diffraction patterns in Fig. 3 were taken.

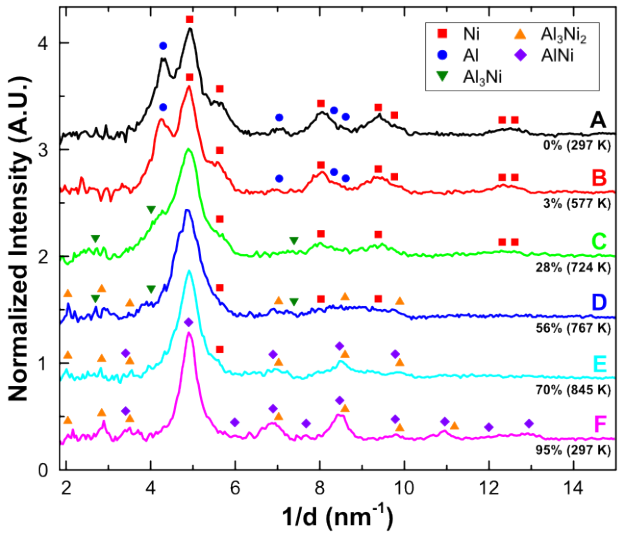

Fig. 3 – DTEM electron diffraction patterns captured before, during, and after the reaction of a 100 nm Al/Ni bilayer. The pattern labels correspond to those in Fig. 2. Also labeled for each pattern are the percentage of heat released (as a fraction of the theoretical enthalpy of formation) and the temperature when the pattern was captured.